MCB
Journals.ASM.org

Retinol-Binding Protein 4 and Its Membrane Receptor STRA6 Control Adipogenesis by Regulating Cellular Retinoid Homeostasis and Retinoic Acid Receptor α Activity

Matthias Muenzner,[a] Neta Tuvia,[a] Claudia Deutschmann,[a] Nicole Witte,[a] Alexander Tolkachov,[a] Atijeh Valai,[b] Andrea Henze,[c] Leif E. Sander,[b] Jens Raila,[c] Michael Schupp[a]

Department of Endocrinology, Diabetes, and Nutrition and Center for Cardiovascular Research, Charité University Medicine, Berlin, Germany[a]; Department of Infectious Diseases and Pulmonary Medicine, Charité University Medicine, Berlin, Germany[b]; Department of Physiology and Pathophysiology, Institute of Nutritional Science, University of Potsdam, Nuthetal, Germany[c]

Retinoids are vitamin A (retinol) derivatives and complex regulators of adipogenesis by activating specific nuclear receptors, including the retinoic acid receptor (RAR) and retinoid X receptor (RXR). Circulating retinol-binding protein 4 (RBP4) and its membrane receptor STRA6 coordinate cellular retinol uptake. It is unknown whether retinol levels and the activity of RAR and RXR in adipocyte precursors are linked via RBP4/STRA6. Here, we show that STRA6 is expressed in precursor cells and, dictated by the apo- and holo-RBP4 isoforms, mediates bidirectional retinol transport that controls RARα activity and subsequent adipocyte differentiation. Mobilization of retinoid stores in mice by inducing RBP4 secretion from the liver activated RARα signaling in the precursor cell containing the stromal-vascular fraction of adipose tissue. Retinol-loaded holo-RBP4 blocked adipocyte differentiation of cultured precursors by activating RARα. Remarkably, retinol-free apo-RBP4 triggered retinol efflux that reduced cellular retinoids, RARα activity, and target gene expression and enhanced adipogenesis synergistically with ectopic STRA6. Thus, STRA6 in adipocyte precursor cells links nuclear RARα activity to the circulating RBP4 isoforms, whose ratio in obese mice was shifted toward limiting the adipogenic potential of their precursors. This novel cross talk identifies a retinol-dependent metabolic function of RBP4 that may have important implications for the treatment of obesity.

The expansion of adipose tissue in obesity is characterized by an increase in both adipocyte number and size (1). The understanding of factors that control differentiation of precursor cells has significance for the identification of new therapeutic strategies to treat obesity and associated diseases, such as type 2 diabetes.

Retinoic acid receptor (RAR) and retinoid X receptor (RXR) are members of the nuclear receptor family with broad biological functions (2). Both receptors comprise several isotypes and are the molecular targets of retinoid ligands. Recent data suggest an important role for retinoids, their cellular binding proteins (3, 4), and metabolizing enzymes (5, 6) in the control of adiposity. Pharmacological intervention with retinoid ligands such as vitamin A (retinol) (7) or its oxidation products retinaldehyde (5) and all-*trans*-retinoic acid (atRA) (8, 9) reduces body weight and adiposity in rodents, whereas feeding mice a retinol-deficient diet increases their fat mass (10). Although in adipose tissue retinoids regulate a variety of metabolic functions, such as thermogenesis, lipolysis, and fatty acid oxidation (11), a direct action on adipocyte differentiation is likely to contribute to their effects on adiposity (12). Proadipogenic effects of low concentrations of atRA in clonal Ob17 precursor cells, rat preadipocytes, and aldehyde dehydrogenase 1A1 (ALDH1A1)-deficient fibroblasts have been reported (13, 14). However, most studies in adipocyte lineage-committed preadipocytes identified atRA as a strong inhibitor of adipogenesis when present at early stages of differentiation (5, 15–18). These inhibitory effects were found to be mediated by an indirect mechanism involving RARα (17, 18) and inhibition of the proadipogenic transcription factor CCAAT/enhancer-binding protein (C/EBP) (19). Activation of RARα by atRA stimulated the expression of the transforming growth factor β effector protein SMAD3, which reduced C/EBPβ DNA binding by interacting with C/EBPβ via its Mad homology 1 domain (20, 21). Besides RARα, RARγ has also been implicated in the inhibitory effects of atRA on adipocyte differentiation by inducing the expression of delta-like 1 homolog/preadipocyte factor 1 (PREF-1) (9), a potent inhibitor of adipogenesis (22). The endogenous high-affinity ligand for RXRα, 9-*cis* RA (23, 24), blocks differentiation presumably due to the fact that it also binds and activates RARα (5). In contrast, selective RXR activation by synthetic agonists enhanced (25), whereas an RXR antagonist prevented, adipocyte differentiation (26). This is consistent with the notion that RXR is the obligate heterodimeric partner for other nuclear receptors involved in adipocyte differentiation, such as peroxisome proliferator-activated receptor γ (PPARγ) (27). Retinaldehyde, which activates RARα less potently than does atRA or retinol (28), was shown to block adipogenesis by inhibiting RXR and PPARγ activation (5).

The lipid-soluble vitamin retinol is delivered to target cells mainly by two distinct mechanisms: as retinyl esters incorporated in lipoproteins (primarily chylomicrons) by the action of lipoprotein lipase or bound to the specific transport protein for retinol in serum, retinol-binding protein 4 (RBP4; also known simply as

Received 22 February 2013 **Returned for modification** 25 March 2013
Accepted 7 August 2013
Published ahead of print 19 August 2013
Address correspondence to Michael Schupp, michael.schupp@charite.de.
Supplemental material for this article may be found at http://dx.doi.org/10.1128/MCB.00221-13.

doi:10.1128/MCB.00221-13

RBP) (29). RBP4 circulates in a complex with transthyretin (TTR) to prevent renal filtration and catabolism (30) and, after dissociation from TTR (31), binds to STRA6 on target cells, a recently identified RBP4 membrane receptor (32). STRA6 acts as a retinol transporter in the membrane, linking retinol uptake to storage and cellular metabolism in extrahepatic tissues (33). Mice with a disruption in *Stra6* appear normal but are compromised in their visual responses and ocular morphology (34). In contrast, mutations of human *STRA6* cause severe developmental malformations associated with disturbed atRA signaling (35). The reason for these phenotypical differences caused by STRA6 loss of function between mouse and human is currently unknown. In addition to STRA6, another receptor, named RBPR2, has been identified and is thought to mediate the known effect of retinol recycling from serum RBP4 to the liver (36).

Although retinyl ester delivery by lipoproteins is significant in the postprandial state, most cellular retinoids are derived from retinol-bound holo-RBP4 (37). RBP4 itself is secreted from a variety of tissues, mainly from organs that store retinoids such as liver and adipose tissue (38). In the liver, retinoids are stored primarily as retinyl esters in specialized hepatic stellate cells, whereas retinol-bound RBP4 is released by the hepatocyte (39). Circulating RBP4 then coordinates cellular retinoid homeostasis through STRA6 and RBPR2. Interestingly, obesity leads to an increase in circulating RBP4, and elevated levels have been associated with insulin resistance (38). Whether canonical RBP4 signaling and cellular retinoid homeostasis are linked to impaired insulin sensitivity is currently unknown (37, 40). Alternative mechanisms have been identified: a recent report showed that holo- but not apo-RBP4 phosphorylates STRA6, which activates signal transducer and activator of transcription 5 (STAT5) in hepatocytes, thus contributing to the development of insulin resistance by inducing suppressor of cytokine signaling 3 (SOCS3) and PPARγ expression (41, 42). Another study demonstrated that in macrophages, which do not express STRA6, RBP4 induces the expression of proinflammatory cytokines independently of retinol through Toll-like receptor 4 and c-Jun N-terminal kinase (43). In addition, RBP4 was able to enhance the maturation and activity of sterol regulatory element-binding protein 1 by upregulating the PPARγ coactivator 1β (PGC-1β) in human hepatoma cells (44) and induce proinflammatory gene expression in human endothelial cells independently of retinol (45), underlining the complexity of RBP4's cellular actions.

Despite a lot of attention being received for the mature adipocyte as a source of RBP4, the function of STRA6-mediated retinol delivery by RBP4 to adipocyte precursor cells is completely unknown. In all previous studies that have investigated the effects of retinoids on adipogenesis, these compounds were applied, as far as we know, directly to the cell medium. Due to their high lipophilicity, added retinoids readily penetrate the cell membrane, bind intracellular transport proteins, and activate their corresponding nuclear receptors. In contrast, we hypothesized that RBP4 and its membrane receptor STRA6 constitute an additional level of regulation that controls cellular retinoid homeostasis and subsequent differentiation of precursor cells. Indeed, we found that STRA6 is expressed in adipocyte precursors that are located in the stromal-vascular fraction (SVF) of adipose tissue and that a mobilization of hepatic retinoid stores by elevated RBP4 secretion in mice activates RARα signaling in the SVF. Unexpectedly, STRA6 mediated not only retinol influx from holo-RBP4 that blocked adipocyte differentiation by activating RARα but also retinol efflux to apo-RBP4, which enhanced differentiation. The directionality of retinol flux depended on the extracellular RBP4 isoforms. We also found that the RBP4 isoforms were altered in serum of obese mice, favoring a reduction in the adipogenic potential of their precursor cells. Thus, RBP4 and STRA6 are novel regulators of adipocyte differentiation by controlling the availability of nuclear receptor ligands for RARα in precursor cells.

MATERIALS AND METHODS

Cell culture, ligand incubations, and oil red O staining. 3T3-L1 and C3H10T1/2 cells were purchased from American Type Culture Collection and grown to confluence in high-glucose Dulbecco's modified Eagle's medium (DMEM) and Eagle's basal medium with 2 mM L-glutamine, 1.5 g/liter sodium bicarbonate, and Earle's balanced salt solution (BSS), respectively, both supplemented with 10% fetal bovine serum (FBS) and penicillin-streptomycin (all Life Technologies, Germany). Two days postconfluence, differentiation was induced by supplementing with 0.4 μM dexamethasone, 3 μg/ml human insulin, and 0.25 mM 3-isobutyl-1-methylxanthine (all Sigma, Germany) for 2 days. Cells were maintained for an additional 2 days with insulin alone. To achieve submaximal differentiation, cells were incubated with 3-fold-lower concentrations of the inducers (suboptimal conditions). Mouse embryonic fibroblasts (MEFs) were isolated from male C57BL/6J embryonic day 12.5 (E12.5) to E14.5 embryos by removing the head and limbs and homogenizing the body using an 18-gauge syringe. MEFs were cultured in AlphaMem (Sigma) supplemented with 10% fetal bovine serum, glutamine, and penicillin-streptomycin (all Life Technologies) and differentiated similar to 3T3-L1 cells by using 3-fold-higher concentrations of the inducers. BOSC23 and 293A cells were grown in DMEM supplemented with 10% fetal bovine serum and penicillin-streptomycin. All retinoids, including the RARα antagonist AGN 193618 and holo- and apo-RBP4, were added directly to the cell culture medium for the indicated times. To increase the concentration of cellular retinoids, cells were preloaded with 1 μM retinol for 24 h and washed once with phosphate-buffered saline (PBS) before the induction of differentiation (see Fig. 6A). Oil red O staining of adipocytes and the isolation and adenoviral infection of primary mouse hepatocytes were performed as previously described (46, 47).

Animal studies, adenovirus preparations, and tail vein injections. All animal procedures were in accordance with institutional guidelines and approved by the corresponding authorities. Adenoviruses expressing green fluorescent protein (GFP) and murine RBP4 were generated using the Adeno-X Expression System 2 (Clontech) as described previously (48) and purified by standard CsCl gradients. Titers were determined by the Adeno-X rapid titer kit (Clontech). Equal titers ($\sim 1.2 \times 10^9$ inclusion-forming units [IFU]) were injected via the tail vein into male C57BL/6J mice at 2 months of age. Four days earlier, mice chow was replaced by a 60 kcal% fat high-fat/high-sucrose diet (HFD; Research Diets). After 6 days, mice were sacrificed, serum and organs were isolated, and parts of the epididymal fat pad were fractionated by a collagenase digest. For analyzing serum RBP4 isoforms in obese mice, male C57BL/6J wild-type mice were fed an HFD for 10 weeks starting at 6 weeks of age and compared to age-matched mice on a normal chow (NC) diet. Sera of genetically obese *ob*/*ob* mice (at an age of >6 months, kindly provided by Arvind Batra, Department of Gastroenterology, Infectiology and Rheumatology, Charité Hospital, Berlin, Germany) were compared with sera of age-matched wild-type (wt) mice.

Adipose tissue fractionation. Murine epididymal fat pads were removed, cut into small pieces, and digested using 0.1% collagenase type 2 (Sigma) in PBS at 37°C for 1 h with vigorous shaking at 180 rpm. The cell suspension was filtered through a 250-μm-pore-size Nylon mesh to remove undigested tissue. The precleaned suspension was then centrifuged at room temperature at 1,500 rpm for 3 min to separate stromal-vascular and adipocyte fractions. Each fraction was collected, flash-frozen in liquid nitrogen, and stored at −80°C until mRNA preparation.

Fluorescence-activated cell sorting (FACS). To identify specific cell subsets, single-cell suspensions of pooled visceral fat tissue from 4 mice per group were stained with the antibodies as specified below, with thorough washing between stain layers. Flow cytometric cell sorts were performed on an ARIA cell sorter (BD Biosciences) running FACSDiva software and analyzed with FlowJo version 7 (Tree Star). Adipocyte precursor cells were identified among the CD45-allophycocyanin (APC)/CY7$^-$ (BioLegend) cells by binding to CD34-bio (eBioscience), visualized with SA-Brilliant Violet 510 (BioLegend) and CD29-APC (eBioscience). All subsets were sorted with more than 98% purity.

RNA isolation and qPCR. RNA was purified by standard spin column kits (Qiagen, Hilden, Germany, or Macherey-Nagel, Düren, Germany). cDNA was generated using the Sprint Powerscript system or Moloney murine leukemia virus reverse transcriptase (Promega). Quantitative PCRs (qPCR) were carried out by using the TaqMan or Sybr green PCR mastermix (Applied Biosystems, Foster City, CA, or Promega) and evaluated according to the standard curve method. All mRNA expression data were normalized to 36B4 or hypoxanthine phosphoribosyltransferase (HPRT). The sequences of all primers used are listed in Table S1 in the supplemental material.

Immunoblotting and densitometry. Whole-cell proteins were isolated and homogenized by standard methods and separated by SDS-PAGE. Protein concentrations were determined by the bicinchoninic acid (BCA) method (Thermo Scientific). After incubation with antibodies for PPARγ (sc-7273; Santa Cruz, CA), aP2 (2120; Cell Signaling), RBP4 (Dako, Germany), adiponectin (sc-26497; Santa Cruz), total AKT (Cell Signaling), p-STAT5 (9359; Cell Signaling), RAN (BD Biosciences), or β-actin (sc-47778; Santa Cruz), a secondary horseradish-conjugated antibody was added, and a chemiluminescent substrate kit (GE Healthcare) was used for detection. For the determination of STRA6 protein levels, cells were lysed in 40 mM Tris-HCl buffer (pH 7.5) containing 150 mM NaCl, 0.3% NP-40, 10% glycerol, 50 mM NaF, 2 mM Na_3Vo_4, 0.5% Triton, and the complete protease inhibitor cocktail (Roche). Cell lysates were denatured in sample buffer (60 mM Tris HCl [pH 6.8], 1% SDS, 250 mM dithiothreitol [DTT], 10% glycerol) and heated in a 37°C water bath for 5 min. Samples (30 μg total protein) were subjected to extensive separation by 10% SDS-PAGE, transferred to polyvinylidene difluoride (PVDF) membranes, and blocked with 3% nonfat milk in Tween-TBS (0.1% Tween 20). The STRA6 antibody was diluted 1:333 (EB07811; Everest) or 1:500 (H00064220-D01P; Novus/Abnova) in 0.05% Tween-TBS with 4% nonfat milk and incubated for 3 h at room temperature. Native gel electrophoresis to investigate RBP4 isoforms was carried out by diluting cell culture medium, mouse serum, or recombinant RBP4 samples with loading buffer (125 mM Tris HCl [pH 6.8], 20% glycerol, 0.01% bromphenol blue) without boiling, followed by a separation at 4°C on a 12% acrylamide gel that lacks detergents. Densitometric analyses were carried out by ImageJ.

Plasmid cloning, mutagenesis, and retroviral expression. Mouse or human STRA6 coding sequences (Thermo Scientific) were transferred into pMSCV by In-Fusion cloning (Clontech). Site-directed mutagenesis (Stratagene) was used to introduce the T645M point mutation according to the manufacturer's instructions. Retroviral particles were generated in BOSC23 cells and used to infect preconfluent 3T3-L1 cells as previously described (46).

RBP4 production and HPLC purification. Human His-RBP4 was produced in *Escherichia coli* and purified by Ni-nitrilotriacetic acid (NTA)-agarose beads and high-performance liquid chromatography (HPLC) according to a published protocol (49). Apo-RBP4 was obtained by repeated hexane extractions of purified holo-RBP4 and validated by UV spectroscopy and native immunoblotting experiments.

Transfections and luciferase reporter assay. 3T3-L1 cells were transfected by electroporation as described previously (46). RARE or Gal4-RARα-LBD/Gal4-DBD-firefly luciferase reporter activity was normalized to renilla luciferase activity (dual luciferase; Promega). RNA interference (RNAi)-mediated silencing of the STRA6 protein was performed by electroporating preconfluent 3T3-L1 or C3H10T1/2 cells with 3 nmol of small interfering RNA (siRNA) oligonucleotides (see Table S1 in the supplemental material) as previously described (46).

Determination of retinoids. Mouse serum levels of retinol were determined by the clinical chemistry department of Charité Hospital (LaborBerlin). Retinol and retinyl esters in cell pellets, cell supernatants, and liver tissues were determined after organic extraction using a modified gradient reverse-phase HPLC system (Waters, Eschborn, Germany). Samples were resuspended in 200 μl distilled water and sonicated two times for 10 s. To this suspension and to 200 μl of cell culture medium, 200 μl of ethanol and 1 ml of *n*-hexane were added, vortexed for 10 min, and centrifuged (1,500 × *g*; 10 min). Then the upper organic layer was removed. The addition of 1 ml of *n*-hexane was repeated once. The combined *n*-hexane layer was dried under nitrogen (30°C) and resuspended in 200 μl of isopropanol. Retinol and retinyl esters were separated on a C_{30} column (5 μm, 250 by 3.0 mm; YMC, Wilmington, NC). The solvent system consisted of a 60-min linear gradient from solvent A (methanol-water [90/10, vol/vol; 0.4 g/liter ammonium acetate in H_2O]) to solvent B [methanol–methyl-*tert*-butyl-ether–water [8/90/2, vol/vol/vol, with 0.1 g/liter ammonium acetate in H_2O]) as the eluent at a flow rate of 0.2 ml/min. Retinol, retinyl oleate, retinyl palmitate, and retinyl stearate were identified at 325 nm and quantified by comparison of retention time as well as peak areas with external standards using a photodiode array detector (model 996; Waters). Accuracy and precision of the analyses were verified using standard reference material (SMR 968; fat-soluble vitamins in human serum; National Institute of Standards and Technology, Gaithersburg, MD). The coefficients of variation (CV) were 1.6% and 2.5% for retinol and retinyl palmitate, respectively. The recovery was over 97% for retinol and over 92% for retinyl palmitate.

Retinol transport studies. Confluent 3T3-L1 cells (12-well plate) were washed twice with PBS and loaded with 5 nM (4 μCi) [11,12-^{3}H(N)] retinol (PerkinElmer Life Sciences; dissolved in ethanol) in DMEM for 2 h. Cells were then washed twice with PBS and incubated with medium (DMEM only or DMEM supplemented with either 100 μM bovine serum albumin [BSA] or 10% FBS) with BSA or apo-RBP4 as indicated for a certain time period (between 10 and 120 min). Medium was collected and cells were washed twice with PBS before solubilization in 200 μl 1% SDS in PBS. Lysates and medium samples were mixed with Instant Scint-Gel Plus (PerkinElmer Life Sciences) and measured by a scintillation counter. All experiments were done in triplicates.

Statistical analyses. Representative results from at least three independent cell culture experiments are shown and are presented as means ± standard deviations (SD). Animal data are expressed as means ± standard errors of the means (SEM). Significance was determined by the 2-tailed Student *t* test or analysis of variance (ANOVA), as appropriate, and *P* values of <0.05 were deemed significant.

RESULTS

STRA6 is expressed in adipocyte precursor cells and hepatic retinoid mobilization by RBP4-induced RARα signaling in the SVF of adipose tissue in mice. STRA6 is highly expressed in compartments that require retinol, such as the retinal pigment endothelium (RPE) (32, 50), and its deficiency strongly reduces the retinoid content of the RPE (34). As reported earlier (41), STRA6 mRNA was hard to detect in liver and showed low expression in muscle and severalfold higher expression in epididymal white adipose tissue (eWAT) (data not shown). To explore its function in adipose tissue, we first investigated STRA6 mRNA expression in collagenase-digested eWAT of C57BL/6J mice. We found that STRA6 and other components of the retinoid signaling cascade, such as RARα, RARβ2, cellular RBP1 (CRBP1), and CYP26A1, were expressed predominantly in the SVF of adipose tissue, which is known to harbor adipocyte precursor cells (Fig. 1A). Accordingly, CRBP1, STRA6, and also the known precursor cell marker

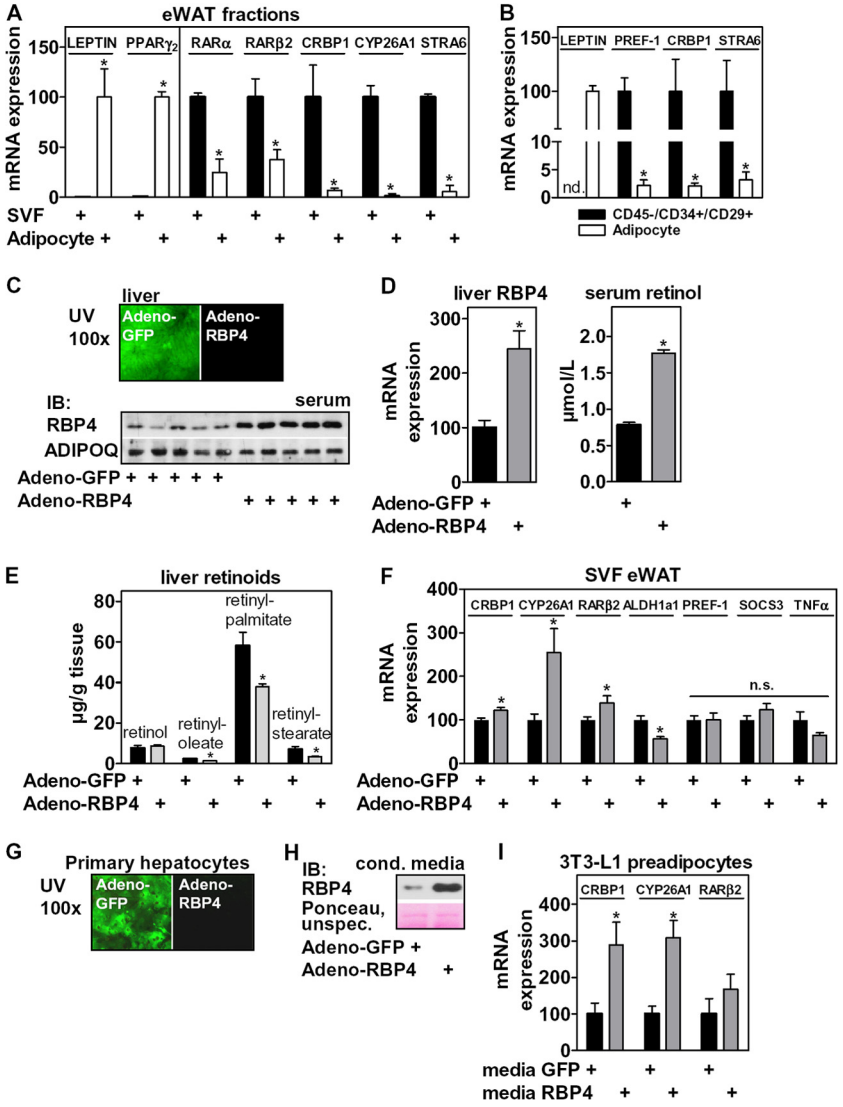

FIG 1 STRA6 is expressed in adipocyte precursor cells, and retinol mobilization by ectopic RBP4 expression in liver induces RARα signaling in the SVF of mice. (A) mRNA expression of adipocyte markers and genes involved in retinoid signaling in collagenase-digested eWAT. (B) Gene expression in the precursor cell population isolated from the SVF of eWAT by FACS. (C) Mice were tail vein injected with GFP- or RBP4-expressing adenoviruses ($n = 9$ mice each) and sacrificed 6 days later. Liver tissues were investigated by UV microscopy and serum by immunoblotting for RBP4 and ADIPOQ. (D) Liver tissues were analyzed for RBP4 mRNA, and serum retinol was measured by HPLC. (E) Liver tissue retinoids were quantitated by HPLC. (F) mRNA expression of several known RARα targets, PREF-1, TNF-α, and SOCS3, were determined in the SVF of injected animals. (G) Primary murine hepatocytes were infected with GFP- or RBP4-expressing adenoviruses and investigated by UV microscopy. (H) After 36 h, conditioned medium was analyzed by immunoblotting for RBP4. (I) Confluent 3T3-L1 preadipocytes were incubated for 24 h with the indicated medium, and mRNA expression of several RARα targets was determined. *, $P < 0.05$.

PREF-1 (51) were highly expressed in the $CD45^-/CD34^+/CD29^+$ precursor cell population (52) (Fig. 1B), which was isolated by fluorescence-activated cell sorting (FACS) from the SVF of eWAT. Expression of adipocyte-specific peroxisome proliferator-activated receptor γ_2 (PPARγ_2) (Fig. 1A) and leptin (Fig. 1A and B) was highly enriched in the adipocyte fraction, as expected.

We next investigated whether hepatic retinoid mobilization by RBP4 affects RAR signaling in the SVF of adipose tissue in mice. Tail vein injection of GFP- or RBP4-expressing adenoviruses, which are cleared specifically by the liver, resulted in an increase in hepatic RBP4 mRNA expression and a corresponding ~2-fold increase in serum (Fig. 1C and D, left), when analyzed 6 days after the injection. Delivering a Flag-tagged control protein by the same adenoviral route resulted in liver-specific expression and absence of Flag reactivity in all other organs tested, such as adipose tissue, kidney, and muscle (data not shown). The elevated RBP4 secretion from the liver was accompanied by an ~2-fold increase in serum retinol levels (Fig. 1D, right), which is consistent with the notion that liver-secreted RBP4 is retinol-bound holo-RBP4 (53). In addition, we measured a significant reduction in the most abundant retinyl esters (Fig. 1E) that account for more than 95% of all retinoid stores in liver (53) in animals with ectopic RBP4 expression. These data indicate that forced expression of RBP4 in the liver triggers a robust mobilization of hepatic retinoid stores to serum retinol. Strikingly, several known RARα target genes were induced in the SVF of eWAT in these mice (Fig. 1F). ALDH1A1

expression, which was previously shown to be negatively regulated by RARα (14), was decreased, whereas expression of the RARγ target gene PREF-1 (9) was not altered. These data suggest that retinoid levels and RARα activity in adipocyte precursor cells within the SVF are linked to RBP4-dependent retinol delivery, likely via its membrane receptor STRA6. Interestingly, mRNA expression of other previously described RBP4 targets, such as suppressor of cytokine signaling 3 (SOCS3) (41) and tumor necrosis factor α (TNF-α) (43), was not induced in the SVF or tended to be downregulated in this model of retinoid mobilization (Fig. 1F). Taken together, these data indicate that retinoid mobilization from the liver by increased RBP4 secretion induces RARα signaling in the SVF of adipose tissue. This hepatocyte-to-adipocyte precursor cell signaling link was also functional *in vitro*, since conditioned medium from primary murine hepatocytes with adenoviral RBP4 overexpression (Fig. 1G and H) induced the expression of several RARα targets in 3T3-L1 preadipocytes (Fig. 1I), an adipocyte lineage-committed clone derived from Swiss albino mouse embryos (54).

STRA6 is expressed in adipocyte precursors, and holo-RBP4 blocked adipocyte differentiation via STRA6-dependent activation of RARα. Since 3T3-L1 cells responded to RBP4, we analyzed STRA6 expression in these cells. We found that STRA6 mRNA was expressed at higher levels in preadipocytes than in adipocytes (Fig. 2A), which is in accordance with its expression pattern in fractionated adipose tissue. PPARγ$_2$ expression showed the expected specificity for adipocytes. In comparison, the expression of the other known retinol transporter, RBPR2, was high in liver, low in the SVF, and almost undetectable in 3T3-L1 cells (qPCR cycle threshold [C_T] values of >35 cycles] [data not shown]), as previously reported (36). We next measured the level of STRA6 protein by immunoblotting. Because the extremely hydrophobic protein tended to precipitate, we adapted our protein preparation. STRA6 depletion in differentiated adipocytes (data not shown) and overexpression in preadipocytes (Fig. 3A) identified the upper band of a doublet as the murine STRA6 protein, which migrated slightly higher than its expected molecular mass of ~73 kDa. The intensity of the lower unspecific band varied with the antibody lot number and the type of protein extract investigated. The STRA6 protein was detected at low levels in preadipocytes and at higher levels in adipocytes (Fig. 2B, left), similar to the expression of the PPARγ protein, increasing continuously during the time course of differentiation and strikingly different than its mRNA levels, which showed the opposite regulation (data not shown). We observed the same distribution of STRA6 protein expression between the SVF and adipocyte fraction (Fig. 2B, right). The inverse correlation between transcript and protein expression pattern was surprising and is contrary to a previous report that showed higher STRA6 mRNA expression in 3T3-L1 adipocytes, using the identical TaqMan qPCR primer system and antibody for quantification (41). We confirmed our findings by using another self-designed STRA6 primer pair (data not shown). In summary, STRA6 is expressed in the SVF of adipose tissue and 3T3-L1 cells, and its mRNA levels decrease and its protein levels increase during differentiation, pointing to additional posttranslational regulation of STRA6 protein levels. This is further supported by our finding that retrovirally expressed STRA6 also yielded higher protein levels in adipocytes despite the similar mRNA levels between preadipocytes and adipocytes (data not shown).

We then investigated the effects of holo-RBP4 on differentiation. Since stage- and dose-specific effects of retinoids on adipocyte differentiation were described (13, 14, 18), we first tested the impact of retinol and atRA on adipocyte conversion of 3T3-L1 cells when present during the initial 4 days of differentiation (Fig. 2C). When added directly to the cell culture medium, both retinol and atRA inhibited differentiation in a concentration-dependent manner, as shown by oil red O staining at day 7 (Fig. 2D). atRA was a much more potent inhibitor than retinol. The inhibitory effect of nanomolar concentrations of atRA is in contrast to previous studies (13, 14) and may be related to our specific treatment period and/or cellular context. In accordance with earlier findings that the inhibitory effect is mediated by RARα, a specific RARα receptor antagonist (55), supplemented during the same period with 4 h of preincubation, rescued differentiation of retinol-treated cells (Fig. 2E). Human His-tagged RBP4 was expressed in *E. coli*, refolded in the presence of excess retinol, and purified by HPLC according to a published protocol (49). Apo-RBP4 was produced by repeated hexane extraction of purified holo-RBP4 and verified by UV spectrometry. RBP4 isoforms were validated by nondenaturing immunoblotting, visualizing specific bands (Fig. 2F). Both holo- and apo-RBP4 protein amounts and degree of retinol association remained constant for 48 h in cell culture medium at 37°C (data not shown), suggesting that the isoforms are stable in cell culture medium. When present during the first 4 days, holo-RBP4 potently blocked differentiation, as assessed by phase-contrast microscopy and oil red O staining of intracellular lipids (Fig. 2G, left). Consistently, expression of the adipocyte-specific marker adipose protein 2 (aP2) was strongly reduced, whereas expression of the preadipocyte-specific marker PREF-1 was increased after 7 days of differentiation (Fig. 2G, right). Holo-RBP4 inhibited differentiation dose dependently at concentrations of ≥200 nM (Fig. 2H). A direct comparison with retinol confirmed its lower potency (data not shown). During a 24-h incubation with preadipocytes, holo-RBP4 also induced the RARα target gene CRBP1 (56) in confluent preadipocytes, suggesting that holo-RBP4 acts through RARα (Fig. 2I). Induction of CRBP1 by holo-RBP4 was concentration dependent, with doses that matched its potency to inhibit differentiation and to activate the RARα ligand-binding domain (LBD) in precursor cells that were electroporated with the corresponding Gal4 reporters (Fig. 2J).

If holo-RBP4 was to activate RARα via retinol uptake mediated by STRA6, then this activation should be reduced in STRA6-depleted cells. To this end, we electroporated STRA6 siRNA into preconfluent 3T3-L1 cells, which led to an ~75% reduction of mRNA expression (Fig. 4A). Since protein levels of STRA6 in preadipocytes were hard to detect, we validated the effect of this siRNA in similarly treated adipocytes, which showed a significant reduction in STRA6 protein levels (data not shown). Both retinol and atRA induced CRBP1 in preadipocytes independently of STRA6. In contrast, holo-RBP4 partially lost its effect in STRA6-depleted cells (Fig. 2K). We then tested whether blocking RARα would render holo-RBP4 inactive toward adipogenesis. The specific RARα antagonist, supplemented during the same period with an additional 4 h of preincubation, completely rescued the inhibitory effects of holo-RBP4 on differentiation (Fig. 2L). These data show that holo-RBP4 blocks differentiation by activating RARα in precursor cells in a STRA6-dependent manner.

Ectopic STRA6 enhanced adipocyte differentiation. We then investigated the effects of STRA6 gain of function during differ-

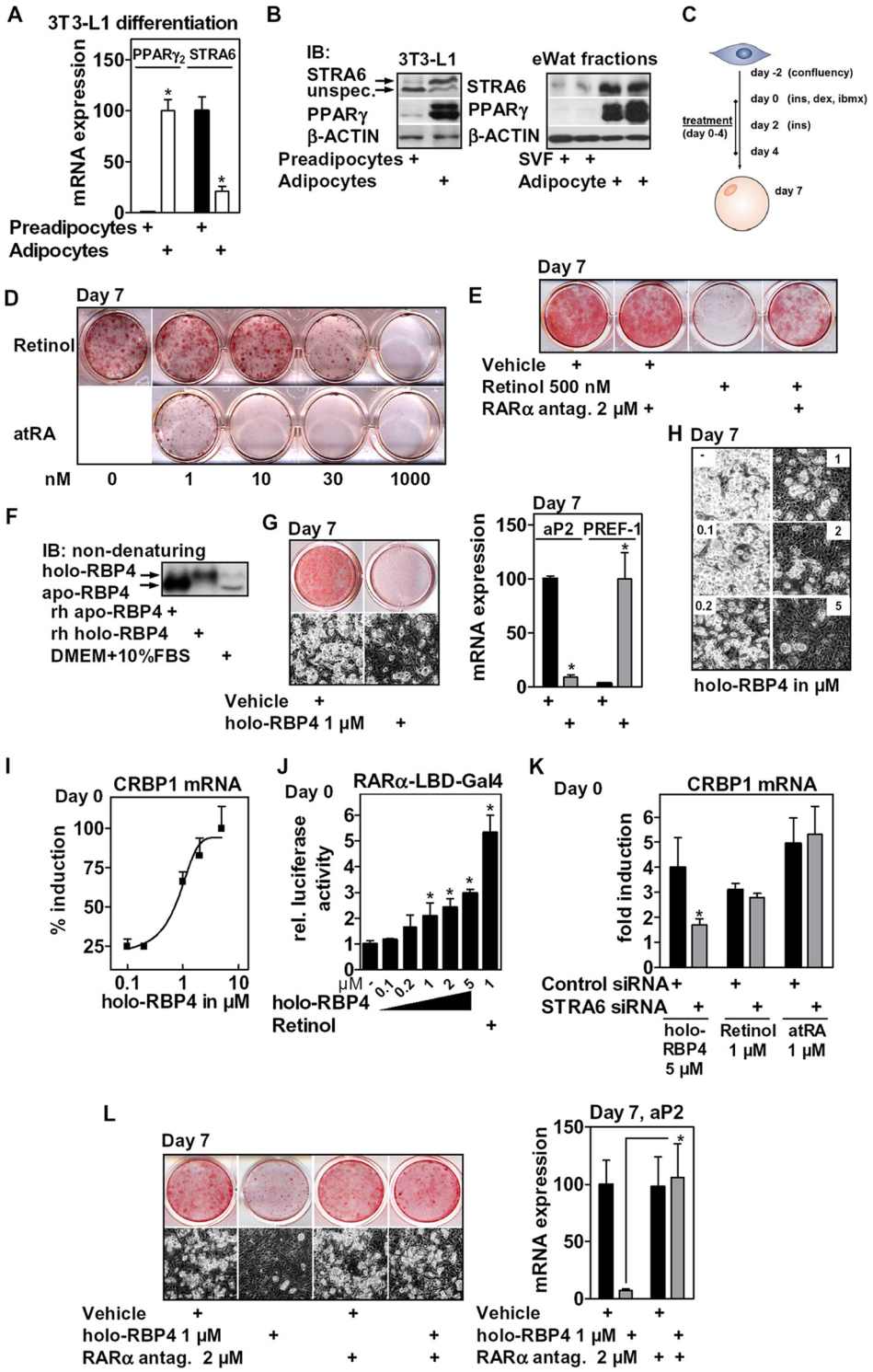

FIG 2 STRA6 is expressed in 3T3-L1 cells, and holo-RBP4 blocks adipogenesis via RARα. mRNA (A) and protein (B, left) expression of PPARγ and STRA6 before and after the differentiation of 3T3-L1 cells (day 0 and day 7) and in collagenase-digested eWAT (B, right) ($n = 2$ mice each). (C) 3T3-L1 cells were differentiated and treated as indicated. (D) Cells were differentiated in the presence of retinoids at the indicated concentrations, and oil red O staining was performed at day 7. (E) Cells were differentiated in the presence of retinol and supplemented with an RARα antagonist (4 h of preincubation). (F) Recombinant human holo- and apo-RBP4 (200 nM) and cell culture medium containing 10% FBS were analyzed by nondenaturing immunoblotting. (G) Adipocyte conversion of holo-RBP4-treated cells was assessed by oil red O staining of intracellular lipids and phase-contrast microscopy (left) and mRNA expression of aP2 and PREF-1 (right). (H) 3T3-L1 cells were differentiated in the presence of increasing concentrations of holo-RBP4 as described for panel G and investigated by phase-contrast microscopy. (I, J, and K) Preadipocytes were treated as indicated for 24 h, and mRNA expression of CRBP1 was determined (I and K); cells were electroporated with RARα-LBD-Gal4 reporters, and luciferase activity was determined (J) or electroporated with control or STRA6 siRNA (K). (L) 3T3-L1 cells were differentiated in the presence of holo-RBP4 as described for panel G, supplementing a specific RARα antagonist (4 h of preincubation). Differentiation was assessed after 7 days. *, $P < 0.05$.

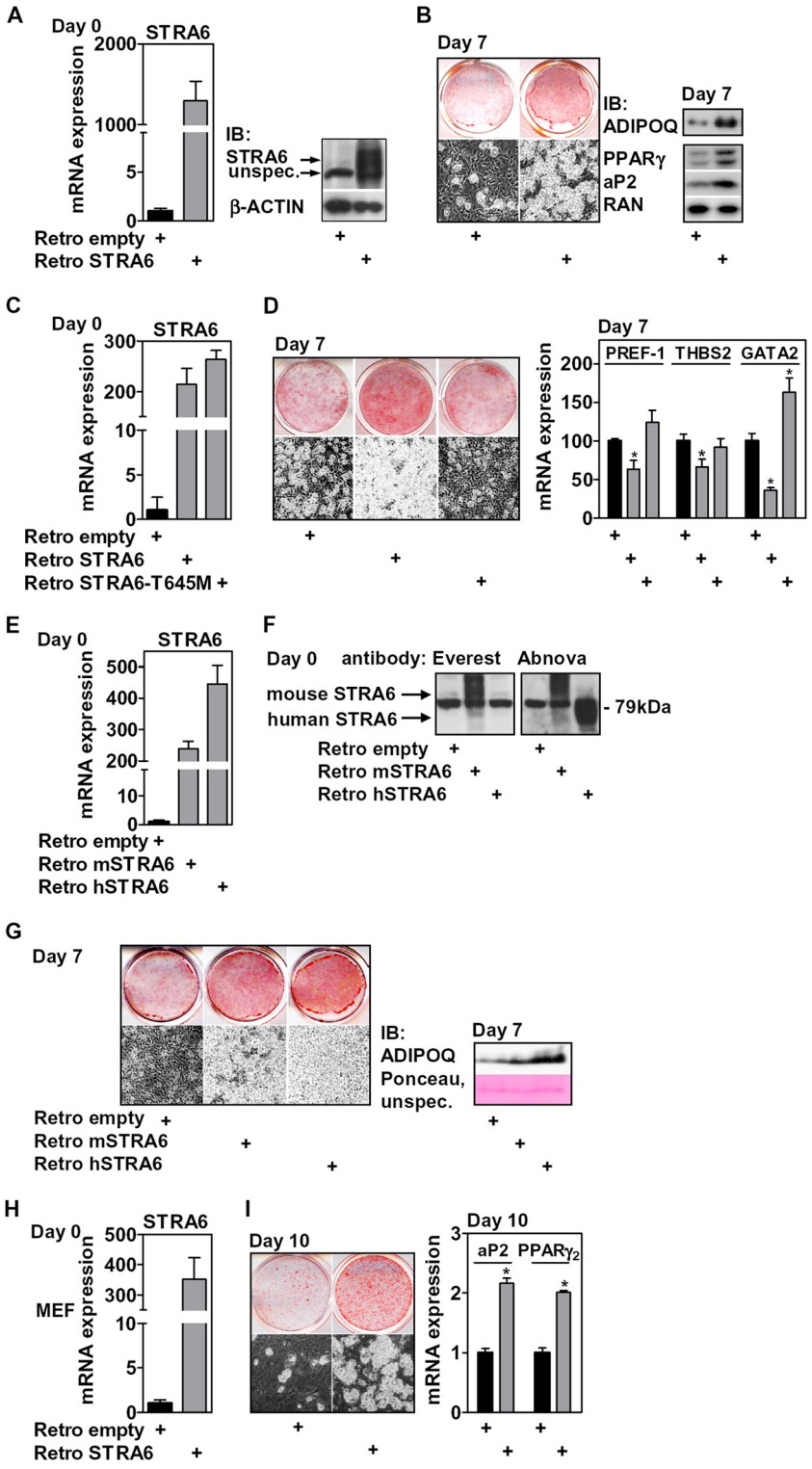

FIG 3 STRA6 overexpression promotes adipocyte differentiation of precursor cells. (A) mRNA and protein expression of retrovirally expressed STRA6 in 3T3-L1 cells at day 0. (B) Adipocyte conversion was assessed 7 days later by phase-contrast microscopy and oil red O staining (left) and protein expression of aP2, PPARγ, and secreted ADIPOQ (right). (C) mRNA expression of retrovirally expressed wt and T645M STRA6 in preadipocytes at day 0. (D) Adipocyte conversion after 7 days of differentiation was assessed by phase-contrast microscopy (left) and mRNA expression of the PREF-1, THBS2, and GATA2 preadipocyte-specific genes (right). (E) mRNA expression of retrovirally expressed mouse or human STRA6 in 3T3-L1 preadipocytes at day 0. (F) Reactivity of the Everest and Abnova antibodies with endogenous mouse and overexpressed mouse and human STRA6 protein at day 0. (G) Cells were induced to differentiate and assessed at day 7 as indicated. (H) mRNA expression of retrovirally expressed STRA6 in MEFs at day 0. (I) Adipocyte conversion was assessed after 10 days. *, $P < 0.05$.

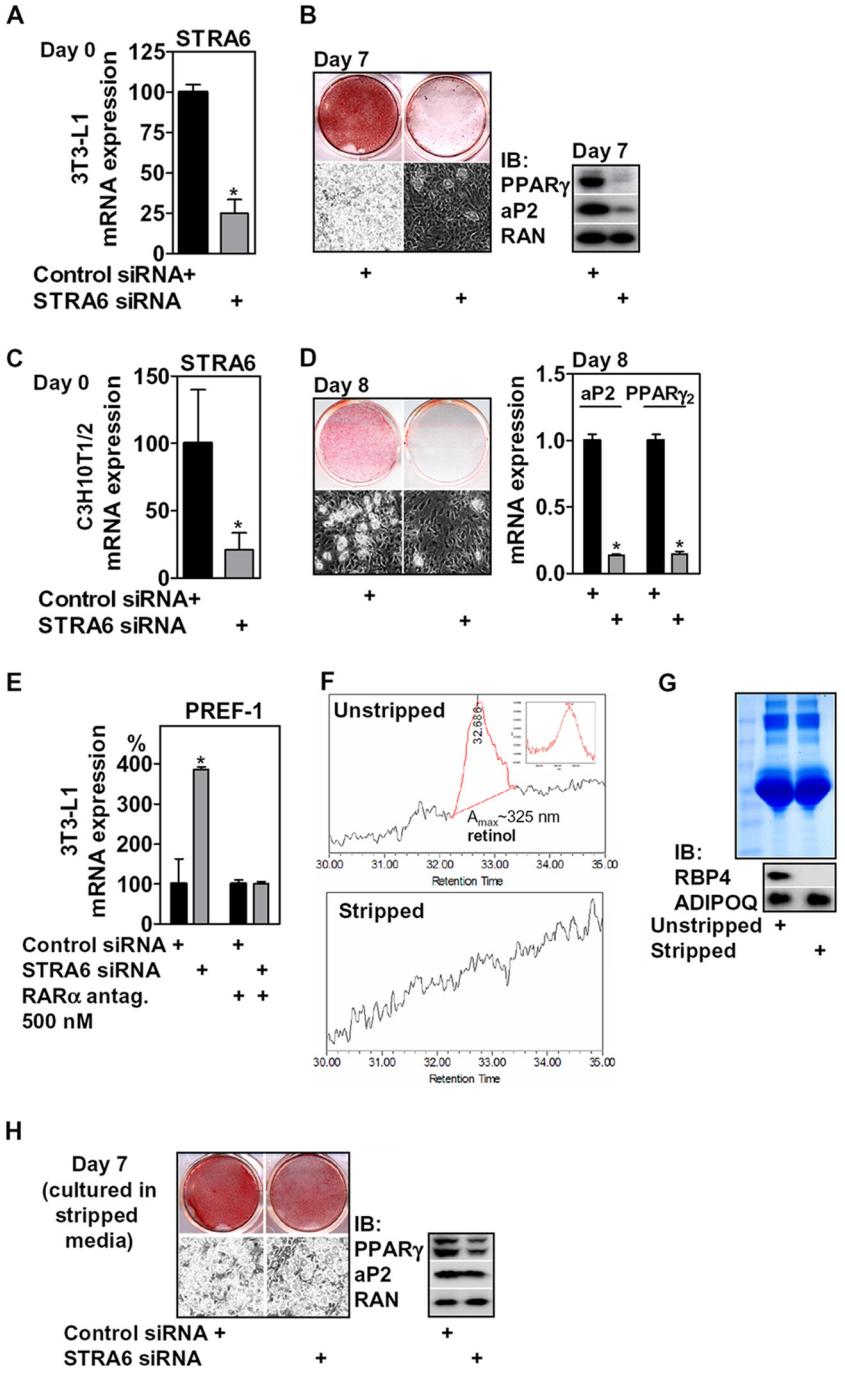

FIG 4 STRA6 depletion inhibits adipogenesis, and this effect depends on RARα and the presence of retinol/RBP4. (A) mRNA expression of STRA6 in 3T3-L1 preadipocytes after electroporation of STRA6 siRNA (day 0); (B) adipocyte conversion was determined 7 days later as indicated. (C) mRNA expression of STRA6 in C3H10T1/2 cells grown to confluence after the electroporation of siRNA oligonucleotides; (D) adipocyte conversion was determined 8 days later as indicated. (E) 3T3-L1 cells were treated as described for panel A and differentiated with or without 500 nM of a specific RARα antagonist supplemented for the first 4 days with 4 h of preincubation before initiating differentiation, and mRNA expression of PREF-1 was determined at day 7 and normalized to control siRNA-treated cells. (F) HPLC analysis of unstripped and charcoal-stripped FBS identifying retinol only in unstripped FBS (inset). (G) Coomassie staining of unstripped and stripped FBS (top) and its protein content of RBP4 and ADIPOQ (bottom). (H) Adipocyte conversion of cells electroporated with STRA6 siRNA and cultivated from day −2 to day 4 in medium containing stripped FBS, assessed at day 7. *, $P < 0.05$.

entiation without the addition of exogenous RBP4. Retroviral expression of STRA6 resulted in a strong increase of both STRA6 mRNA and protein levels at day 0 (Fig. 3A). Differentiation of these cells using a suboptimal differentiation mix (described in Materials and Methods) resulted in low basal differentiation and much enhanced adipocyte conversion in STRA6-overexpressing cells, as shown by oil red O staining, PPARγ and aP2 protein expression, and accumulation of adiponectin (ADIPOQ) in the

cell culture medium, which is secreted exclusively by adipocytes (57) (Fig. 3B). We then asked whether the proadipogenic effects of STRA6 were dependent on its membrane localization. A point mutation of threonine 645 to methionine (T645M; corresponding to T644M of human STRA6) that prevents cell surface expression by interfering with protein folding (58) completely abolished the positive effect of ectopic STRA6 (Fig. 3C) on differentiation, as shown by phase-contrast microscopy, oil red O staining (Fig. 3D, left), and the expression of preadipocyte-specific factors PREF-1, thrombospondin 2 (THBS2), and GATA2 (Fig. 3D, right). The proadipogenic function of STRA6 was not unique to murine STRA6 since overexpression of the human protein (Fig. 3E and F) had the same proadipogenic effect (Fig. 3G). Interestingly, the antibody (Everest) did not recognize the human protein (Fig. 3F), which is in contradiction to a previous study (41). This discrepancy has also been noted by others (40). A different antibody (Abnova), although not sensitive enough to detect endogenous mouse STRA6 protein, gave a strong signal for ectopically expressed mouse and human STRA6, migrating at a slightly different molecular mass (Fig. 3F). STRA6 enhanced differentiation also in primary cells, since mouse embryonic fibroblasts (MEFs) that ectopically expressed STRA6 (Fig. 3H) showed enhanced adipocyte conversion (Fig. 3I). Taken together, our results show that murine and human STRA6, when expressed at the cell surface, enhances adipocyte differentiation.

STRA6 depletion impaired adipocyte differentiation, and its effects were dependent on the presence of retinol/RBP4. As ectopic expression of STRA6 led to enhanced adipocyte differentiation, we investigated whether STRA6 depletion in precursor cells (Fig. 4A) would have the opposite effect. When induced to differentiate, silencing of STRA6 in 3T3-L1 preadipocytes strongly impaired adipocyte conversion and triglyceride accumulation (Fig. 4B). Similarly, STRA6 depletion in pluripotent C3H10T1/2 fibroblasts (Fig. 4C) that can also undergo adipocyte differentiation (59) showed the same results (Fig. 4D). We then asked whether this differentiation defect is linked to RARα receptor activation. Supplementing the specific RARα receptor antagonist, from 4 h before the initiation of differentiation until day 4, prevented the inhibitory effects of STRA6 depletion, as indicated by the expression of PREF-1 after 7 days of differentiation (Fig. 4E). These data indicate that STRA6 requires retinol and RBP4 to affect differentiation. We found that HPLC analysis of FBS-containing cell culture medium consistently identified a peak corresponding to retinol, at a concentration of ~30 nM (Fig. 4F) that corresponded to the levels of bovine holo-RBP4 determined by immunoblotting (Fig. 2F). Charcoal stripping of FBS completely removed this retinol peak (Fig. 4F). Surprisingly, bovine RBP4 was detected only in unstripped but not in stripped FBS (Fig. 4G). We found comparable unspecific Coomassie staining of unstripped and stripped FBS and equal levels of bovine ADIPOQ (Fig. 4G), indicating that stripping did not affect the overall amount of serum proteins. Decreasing the stability of RBP4 by retinol removal or charcoal binding may have caused this depletion. When preadipocytes were cultured from the time of confluence (day −2) until day 4 in stripped medium, the inhibitory effects of STRA6 depletion on differentiation were attenuated (Fig. 4H), indicating that either or both retinol and RBP4 are required for STRA6 to affect differentiation.

STRA6 mediates apo-RBP4-dependent retinol efflux. The proadipogenic effects of STRA6 were unexpected and not compatible with a model in which STRA6 mediates only retinol influx from holo-RBP4, thereby blocking differentiation. Since RBP4 binding to STRA6 has previously been shown to activate STAT5 (41), a proadipogenic transcription factor (60), we first tested whether RBP4 and STRA6 could activate STAT5 signaling in preadipocytes. Only growth hormone (GH), a known activator of STAT5, but not holo-RBP4, apo-RBP4, or retinol at a concentration of 1 μM, was able to induce STAT5 phosphorylation in control or STRA6-overexpressing cells (Fig. 5A). Moreover, there was no induction of PPARγ or SOCS3 mRNA in STRA6-overexpressing preadipocytes (Fig. 5B), and holo- or apo-RBP4 could not induce PPARγ mRNA (data not shown), indicating that STAT5 activation is unlikely to mediate STRA6-induced differentiation. We then tested whether STRA6 could work in conjunction with retinol-free apo-RBP4, which is present in serum-containing culture medium (Fig. 2F). Preadipocytes were electroporated with an RAR response element (RARE) luciferase reporter, preloaded with either vehicle or retinol for 24 h in order to increase the cellular retinoid content, washed, and incubated with retinol or different RBP4 isoforms for an additional 24 h. We found that apo-RBP4 significantly reduced luciferase activity in cells with a retinol preload, whereas holo-RBP4 had no discernible effect in this assay (Fig. 5C). Furthermore, apo-RBP4 significantly repressed the mRNA levels of the RARα targets CRBP1, CYP26A1, and SMAD3 in retinol preloaded cells (Fig. 5D), and this repression was further enhanced by ectopic STRA6 (Fig. 5E). We found that apo-RBP4 strongly reduced the cellular content of retinol and retinyl palmitate (Fig. 5F, left) by repartitioning retinol into the extracellular space (Fig. 5F, right), as evidenced by HPLC. In order to study the transport characteristics, 3T3-L1 preadipocytes were loaded with ^{3}H-retinol, washed, and incubated with apo-RBP4, and the distribution of radioactivity was determined. We found that 1 μM apo-RBP4 induced robust retinol efflux much more potently than bovine serum albumin (BSA), a protein that is known to also bind and transport retinol (61, 62) (Fig. 5G). Even in the presence of 100 μM BSA or 10% FBS, both of which repartitioned significant amounts of retinol to extracellular cell space, 1 μM apo-RBP4 further increased retinol efflux (Fig. 5G). The efflux was concentration dependent (Fig. 5H) and strongly increased by ectopic STRA6 expression (Fig. 5I). We conclude that apo-RBP4 together with STRA6 constitute a potent retinol efflux system in these cells. This efflux system effectively decreases the intracellular availability of retinol-derived nuclear receptor ligands for RARα in precursor cells.

Apo-RBP4 promotes adipocyte differentiation in a STRA6-dependent manner. Since apo-RBP4 reduced RARα activity, we tested whether it also enhances adipocyte differentiation. Preadipocytes were preloaded with retinol and differentiated in the presence of apo-RBP4 as shown in Fig. 6A, left. Retinol preload, very likely due to its RARα-activating effects (Fig. 5C), reduced adipocyte differentiation. Adding apo-RBP4 strongly increased differentiation of these cells, as shown by oil red O staining, phase-contrast microscopy, and the expression of aP2 and PREF-1 at day 7 (Fig. 6A, middle and right). This induction of adipogenesis by apo-RBP4 was concentration dependent (Fig. 6B), with doses matching those at which retinol efflux was observed (Fig. 5H). The same enhancement of differentiation by apo-RBP4 was found in C3H10T1/2 cells (data not shown). This proadipogenic effect was partially blunted in STRA6-depleted cells (Fig. 6C), indicating that STRA6 is required for the proadipogenic effect of apo-RBP4.

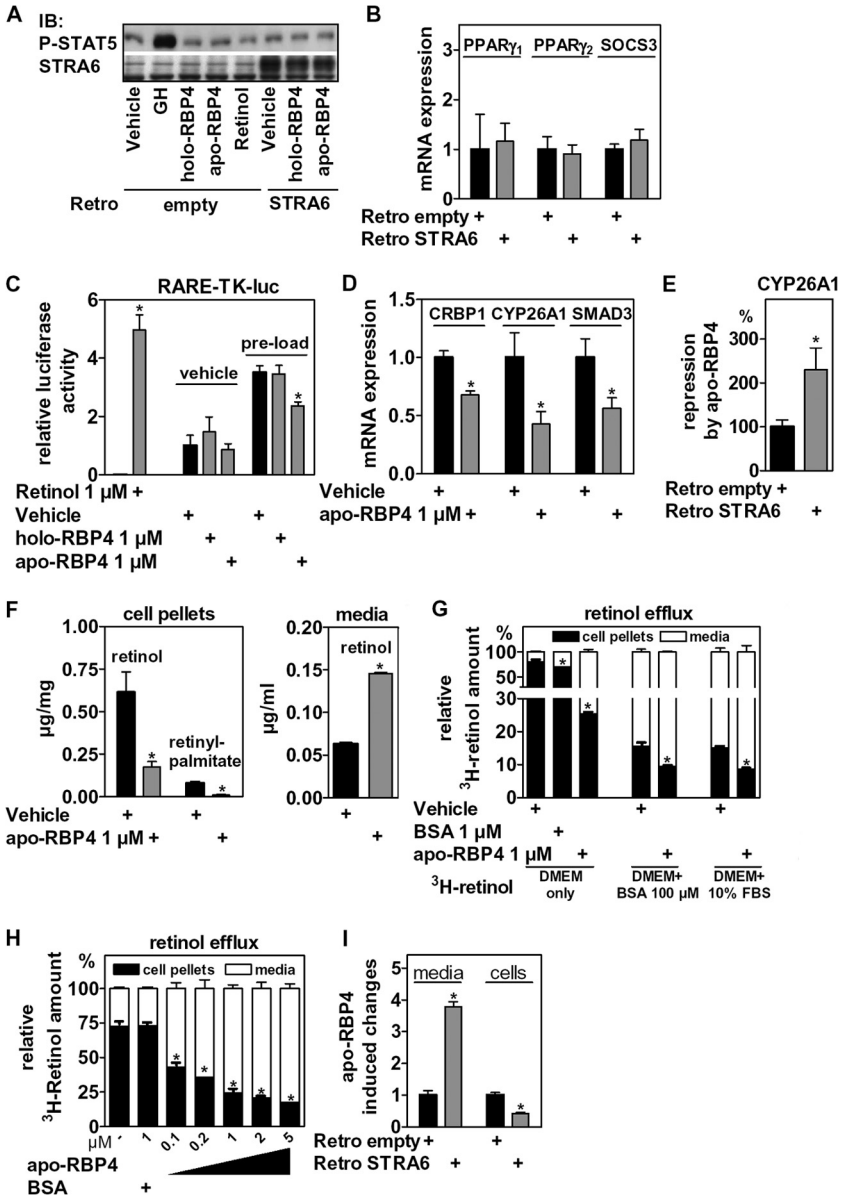

FIG 5 STRA6 and RBP4 in precursor cells work independently of STAT5 signaling by regulating retinoid homeostasis and RARα activity. (A) Confluent 3T3-L1 preadipocytes with control or STRA6 overexpression were stimulated for 20 min with GH (500 ng/ml) or the indicated compound at 1 μM and analyzed for the expression of Tyr694-phosphorylated STAT5 protein. (B) mRNA expression of PPARγ$_1$, PPARγ$_2$, and SOCS3 of control and STRA6-overexpressing cells before the induction of adipocyte differentiation (day 0). (C) 3T3-L1 preadipocytes were electroporated with a RARE-luc reporter, incubated with vehicle or retinol overnight, washed once with PBS, and stimulated with RBP4 isoforms as indicated. (D to F) Confluent 3T3-L1 cells were preloaded with 1 μM retinol overnight, washed once, and incubated with vehicle or apo-RBP4 for 24 h and analyzed for mRNA expression of RARα target genes (D), the fold repression of CYP26A1 mRNA by apo-RBP4 with additional ectopic STRA6 expression (E), and the cellular amount of retinol and retinyl-palmitate (left) and the concentration of accumulated retinol (right) in cell culture medium determined by HPLC (F). (G) 3T3-L1 preadipocytes were loaded with ^{3}H-retinol, washed twice, and incubated as indicated for 2 h, and cellular and supernatant radioactivity was determined. (H) 3T3-L1 preadipocytes were treated as described for panel G and incubated with different concentrations of apo-RBP4 in DMEM only. (I) 3T3-L1 with control or STRA6 overexpression were treated as described for panel G and incubated with 1 μM apo-RBP4 for 10 min in DMEM only. *, $P < 0.05$.

In support of functional epistasis, we found that retinol-preloaded cells differentiated even better with combined apo-RBP4 and ectopic STRA6 expression (Fig. 6D).

Serum RBP4 isoforms are altered in obese mice. RBP4 serum levels are elevated in obesity, which is thought to be due to increased secretion of RBP4 from adipose tissue (38, 63) and to alterations in its association with TTR, which controls renal clearance (64, 65). Considering the opposing effects of holo- and apo-RBP4 isoforms on RARα signaling and adipocyte differentiation, we next investigated whether RBP4 isoform ratios were altered in sera of obese mice (body weights of *ob*/*ob* versus wt mice, 56.2 g ± 4.6 g versus 32.2 g ± 2.7 g; HFD-fed versus normal chow [NC]-fed mice, 43.0 g ± 1.5 g versus 28.0 ± 0.4 g). We visualized the RBP4 isoforms in mouse serum by nondenaturing immunoblotting.

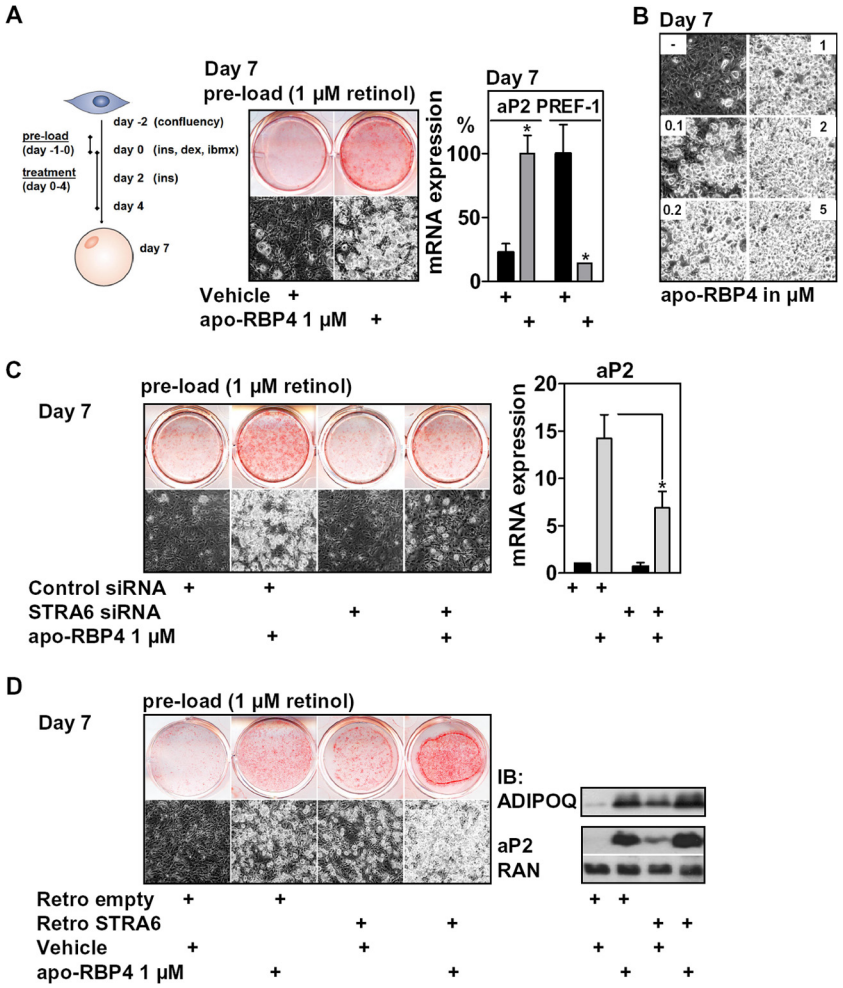

FIG 6 Apo-RBP4 enhances adipocyte differentiation in a STRA6-dependent manner. (A) 3T3-L1 cells preloaded with retinol were differentiated and treated with apo-RBP4 during the first 4 days of differentiation, as depicted. Adipocyte conversion was evaluated after 7 days. (B) 3T3-L1 cells were treated as described for panel A using different concentrations of apo-BP4. (C) 3T3-L1 cells with or without STRA6 depletion were treated as described for panel A, and adipocyte conversion was assessed after 7 days. (D) 3T3-L1 cells with or without retrovirally expressed STRA6 were treated as described for panel A, and adipocyte conversion was assessed after 7 days. *, $P < 0.05$.

Adenoviral expression of murine RBP4 in primary hepatocytes led to an accumulation of both RBP4 isoforms in cell culture medium, validating the detection of both isoforms in serum (Fig. 7A). In addition, hexane extraction of mouse serum, although less efficient than extracting recombinant holo-RBP4, resulted in the expected depletion of holo-RBP4 with a concomitant increase in apo-RBP4 (Fig. 7B). We found an approximately 3-fold increase of total serum RBP4 in obese *ob*/*ob* mice compared to that of wt mice of a similar age (Fig. 7C), as reported previously (38). Despite some variations between animals of the same group, serum samples of *ob*/*ob* mice showed a significantly increased ratio of holo- to apo-RBP4, as quantified by densitometry (Fig. 7C). In order to determine whether this effect was restricted to this particular genetic model, we also analyzed serum samples of mice with diet-induced obesity. Mice fed an HFD for 10 weeks also exhibited increased levels of total RBP4 compared to those of mice fed an NC diet that consisted of increased holo-RBP4 with overall reduced levels of apo-RBP4 (Fig. 7D), similar to *ob*/*ob* mice. Taken together, these data suggest that the elevated levels of RBP4 in the serum of obese mice are accounted for by increased amounts of holo-RBP4.

DISCUSSION

We have discovered that the RBP4 membrane receptor STRA6 is expressed in adipocyte precursor cells and have linked serum RBP4 to the control of retinoid homeostasis in these cells. These findings identify a novel signaling mechanism between hepatocytes and adipocyte precursor cells. We show that mobilizing hepatic retinoid stores by forced RBP4 expression in liver increased the levels of circulating RBP4 with a concomitant increase in serum retinol and induced RARα signaling in the SVF. This finding is physiologically relevant given the high sensitivity of adipocyte precursor differentiation to the activity of RARα. When supplemented in cell culture medium, holo-RBP4 blocked the differentiation of adipocyte precursor cells by activating RARα in a STRA6-dependent manner. These data suggest that retinol can be delivered from hepatic stores to adipocyte precursor cells via RBP4 and STRA6, thus increasing the amount of RARα nuclear

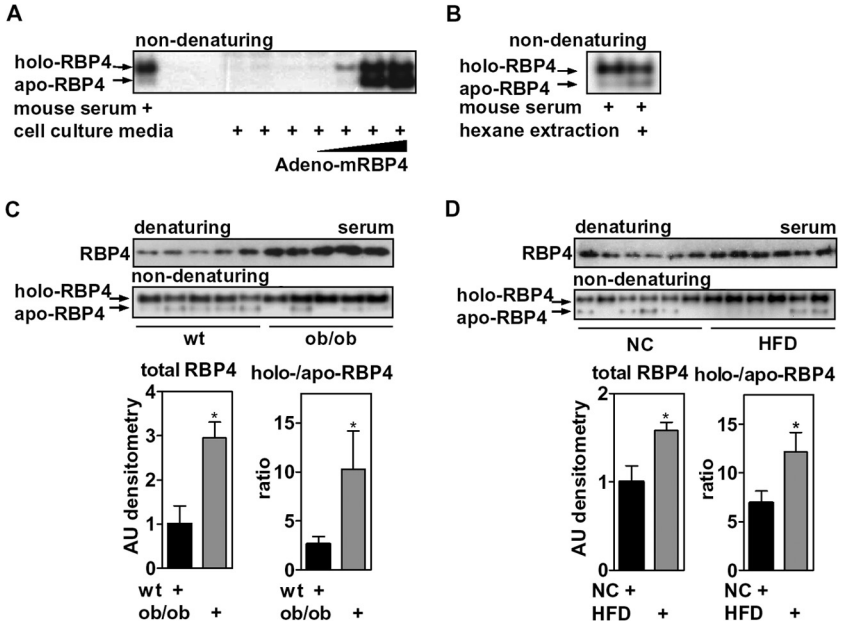

FIG 7 Elevated levels of circulating RBP4 in obese mice are due to increased holo-RBP4. (A) Primary mouse hepatocytes were infected with increasing titers of an adenovirus that expresses murine RBP4. Cell culture medium was analyzed 48 h later by nondenaturing immunoblotting for RBP4 and compared with mouse serum. (B) Mouse serum with or without hexane extraction was investigated by nondenaturing immunoblotting for RBP4. (C) Serum samples of wt and *ob*/*ob* mice ($n = 5$ mice each) were investigated by gel electrophoresis, probed for RBP4 (top) and evaluated by densitometry (bottom). (D) Similar analyses of serum samples from mice on an NC diet or an HFD ($n = 6$ mice each). *, $P < 0.05$.

receptor ligands that inhibit adipogenesis. Surprisingly, we found that STRA6, under standard cell culture conditions, promotes adipogenesis. This was independent of the previously shown activation of STAT5 by RBP4 and STRA6 (41). Instead, we found that its ligand RBP4, when present in its retinol-free apo form, enhances differentiation by potently decreasing RARα activity through retinol efflux, which reduces cellular retinoid levels. We also show that apo-RBP4 loses its proadipogenic potential in STRA6-depleted cells. These findings are in accordance with elegant biochemical studies showing that STRA6 catalyzes not only retinol influx but also efflux and exchange (40, 66), depending on the presence of specific intra- and extracellular retinol-binding proteins. We show that STRA6 depletion inhibits differentiation by increasing RARα activity, which could be due to an accumulation of retinoids, or by disturbing retinol exchange. The latter process is thought to replenish intracellular CRBP1-bound retinol using extracellular holo-RBP4 (40), and interference would increase the cellular content of oxidation products of retinol, such as the more potent RARα activator atRA. STRA6 overexpression enhances differentiation very likely by inducing retinol efflux to apo-RBP4, since we show that apo-RBP4 is present in cell culture medium and that ectopic STRA6 expression resulted in a robust increase in retinol efflux and a more profound repression of the RARα target gene, CYP26A1, in the presence of apo-RBP4. Thus, in addition to cellular retinol uptake, STRA6 catalyzes retinol efflux of intracellular retinoids from precursor cells, thereby alleviating antiadipogenic RARα activity. This homeostatic regulation may be even more relevant *in vivo* since serum levels of RBP4 and retinol are in the low μM range in mice (~0.8 μM retinol) (Fig. 1D) and in humans (between 1.5 and 2.7 μM retinol in humans) (43, 67–69), which is much higher than in *in vitro* cell culture, where retinol is derived entirely from the 10% FBS supplement. Since mature adipocytes, in contrast to precursor cells, couple retinol uptake to the storage of significant amounts of both retinol and retinyl esters (70), STRA6 may have other functions in these cells.

Intriguingly, atRA was shown to drive the commitment of embryonic stem cells to the adipocyte lineage (69, 71–73) and induced expression of the determination factor zinc finger protein 423 (14). Since terminal differentiation of these committed preadipocytes would be blocked by high levels of atRA, an efflux system that reduces intracellular atRA and its precursors after commitment would be required. Therefore, STRA6-mediated retinol efflux, in addition to the regulation of atRA-generating and -inactivating enzymes, such as ALDH1A1 (14) and CYP26A1 (74), is likely to be an important mechanism to fine-tune retinoid levels and RARα activation in precursor cells. Moreover, the strong transcriptional upregulation of STRA6 by retinoids in adipocyte precursor cells (data not shown) may work as a negative feedback that facilitates retinol efflux to prevent excessive receptor activation. These findings are also consistent with a study that investigated the function of STRA6 in zebrafish. Although STRA6 depletion in zebrafish caused retinol deprivation of the developing eye, the authors also observed dysregulated RAR signaling due to retinol excess that caused massive malformations in several embryonic tissues (66). Thus, STRA6 may catalyze retinol influx or efflux in a cell- and tissue-specific manner.

As reported previously, RBP4's induction of STAT5 activity was dependent on STRA6 and retinol transport (41, 42), whereas the induction of inflammatory genes in macrophages and endothelial cells and the induction of PGC-1β in hepatoma cells were not (43, 45). In contrast, we show that RBP4's impact on adipogenesis was dependent not only on STRA6 and retinol transport but also on the nuclear receptor RARα, since the effects of both holo-RBP4 and STRA6 depletion could be rescued by providing a

specific RARα antagonist. This indicates that the variety of RBP4's cellular actions is determined by whether or not the target cell expresses potential mediators, such as TLR4 (43) or STRA6, alone or in combination with other components of the canonical retinoid signaling pathway.

Since RBP4 is secreted also by mature adipocytes, our findings reveal a novel para- and/or endocrine feedback signal to precursor cells. Depending on the resulting isoform of adipocyte-secreted RBP4, this could be either negative or positive feedback on differentiation. The dynamics of RBP4 secretion by adipocytes, and how it couples to systemic retinoid homeostasis, are still unknown and need to be addressed by further research.

At this point, we can only speculate on the relevance of this mechanism for *in vivo* adipocyte differentiation. It is, however, important to note that findings from *in vitro* adipocyte differentiation studies with other factors involved in retinoid metabolism, such as ALDH1A1 and CRBP1, predicted adipose tissue enlargement of the corresponding knockout mice fed an HFD (3, 5). Metabolic studies of STRA6-deficient mice are still lacking. Taking the multifaceted effects of human STRA6 mutations into account, developmental effects may interfere with a phenotype in adipose tissue, and other, yet unknown retinol transporters may compensate for STRA6 deficiency. Similarly complex is the interpretation of genetic mouse models of its ligand RBP4. Mice deficient in RBP4 protein show a deterioration of their retinal function only after insufficient dietary intake of retinol, indicating that RBP4 is dispensable for the peripheral delivery of retinol under standard conditions (29). Furthermore, these mice increase fat mass upon an HFD feeding, similar to control mice (75), suggesting an appropriate adipogenic potential of their precursor cells. Long-term fenretinide treatment, which lowers RBP4 serum levels (38), decreased the fat mass gain of mice on an HFD independent of RBP4 (75), likely by a direct activation of RARα (76). However, our findings suggest that the ratio of holo- to apo-RBP4, rather than the total amount, determines its impact on adipocyte differentiation. Therefore, mice with genetically or pharmacologically induced alterations of this isoform ratio would be more suitable to address the relevance for STRA6 and RBP4 in *in vivo* adipocyte differentiation.

Human serum, in which 13 to 17% of the total RBP4 was found to be apo-RBP4 (68, 69), favored retinol uptake in STRA6-transfected COS-1 cells that coexpressed lecithin-retinol acyltransferase or CRBP1 (40). However, we believe that small changes in the holo- to apo-RBP4 can chronically affect STRA6-mediated retinol transport/exchange and retinoid homeostasis in target tissues *in vivo*. Studies that differentiate between circulating apo-and holo-RBP4 are rare; however, several studies found that the retinol/RBP4 ratio is decreased in sera of obese humans, indicating an elevation in apo-RBP4 (43, 67, 77). Surprisingly, we found that elevated RBP4 serum levels in obese mice consist of holo-RBP4. This apparent conflict could be explained by species differences or, more likely, by the fact that we visualized the apo- and holo-RBP4 isoforms directly instead of calculating the retinol/RBP4 ratio. We believe that the calculated ratio may not necessarily reflect the circulating RBP4 isoforms since, for instance, RBP4-deficient mice still contain more than 12% of the serum retinol found in their wt littermates (29) and the molar concentration of serum retinol can be higher than that of RBP4 in humans (43), suggesting that RBP4-independent retinol transport may also be dynamically altered. Further studies are warranted to account for these differences and to identify the cause for the selective increase of holo-RBP4 levels in serum of obese mice.

Although an increase in fat mass and obesity is clearly a risk factor for the development of insulin resistance, an enhanced adipogenic potential can improve insulin sensitivity by preventing extraadipose tissue fat deposition (3, 78, 79). Hence, the increase of circulating holo-RBP4 in obese mice may reduce the adipogenic potential of precursor cells and prevent further adipose tissue hyperplasia, thereby further decreasing insulin sensitivity by extraadipose tissue fat deposition. RBP4-driven retinoid mobilization in our model, which is unlikely to have a substantial impact on adipose tissue plasticity because of its short duration, did not impair insulin sensitivity (determined by a glucose tolerance test; data not shown). On the other hand, injection of recombinant RBP4 impaired insulin sensitivity in mice after only 7 h, as determined by insulin receptor and AKT1 phosphorylation in skeletal muscle and WAT (41). This indicates that elevated RBP4 in the context of physiological retinol mobilization from the liver greatly differs in its effects on insulin sensitivity from those elicited by injected RBP4. The lack of SOCS3 and TNF-α induction in the SVF by elevated serum RBP4 levels in our model of retinol mobilization underline these important differences. Further studies are required to understand the therapeutic potential of targeting RBP4-mediated retinoid mobilization in regard to the control of adiposity and insulin sensitivity.

In summary, our data show that STRA6 is expressed in adipocyte precursor cells and that RBP4-mediated retinoid mobilization from the liver in mice induces RARα signaling in the SVF, identifying a novel signaling link. STRA6 mediates bidirectional retinol transport that is dictated by the RBP4 isoform ratio and determines the activity of antiadipogenic RARα. Thus, we have identified RBP4 and STRA6 as novel regulators of adipocyte differentiation by controlling retinoid homeostasis and nuclear receptor ligand availability in precursor cells.

ACKNOWLEDGMENTS

This work was supported by the German Research Foundation (DFG; Emmy Noether grant SCHU 2546/1-1 to M.S. and Emmy Noether grant SA1940/2-1 to L.E.S.) and a Career Integration grant from the European Union (CIG 291867 to M.S.). A.T. was supported by the Einstein Foundation Berlin (grant no. A-2010-83 to M.S.).

We acknowledge the Gene Therapy Resource Program of the National Heart, Lung, and Blood Institute, National Institutes of Health (USA), and the University of Pennsylvania Vector Core for providing some of the adenoviral particles used in this study and the assistance of the FCCF at the Deutsches Rheuma-Forschungszentrum, Berlin, Germany. We thank Stefan Weger (Institute of Virology, Charité Hospital, Berlin, Germany) for technical advice on CsCl purification of adenoviral preparations. We thank Robert Hurwitz and Ralf Winter (Max Planck Institute for Infection Biology, Berlin, Germany) for technical help on RBP4 production and Hui Sun (University of California, Los Angeles) for plasmids and helpful discussions. We also thank Lorraine J. Gudas and Moo-Jin Suh (Cornell University, Ithaca, NY) for analyzing retinol in fetal bovine serum.

REFERENCES

1. **Spalding KL, Arner E, Westermark PO, Bernard S, Buchholz BA, Bergmann O, Blomqvist L, Hoffstedt J, Naslund E, Britton T, Concha H, Hassan M, Ryden M, Frisen J, Arner P.** 2008. Dynamics of fat cell turnover in humans. Nature **453:**783–787.
2. **Chambon P.** 1996. A decade of molecular biology of retinoic acid receptors. FASEB J. **10:**940–954.

3. **Zizola CF, Frey SK, Jitngarmkusol S, Kadereit B, Yan N, Vogel S.** 2010. Cellular retinol-binding protein type I (CRBP-I) regulates adipogenesis. Mol. Cell. Biol. **30:**3412–3420.
4. **Zizola CF, Schwartz GJ, Vogel S.** 2008. Cellular retinol-binding protein type III is a PPARgamma target gene and plays a role in lipid metabolism. Am. J. Physiol. Endocrinol. Metab. **295:**E1358–E1368.
5. **Ziouzenkova O, Orasanu G, Sharlach M, Akiyama TE, Berger JP, Viereck J, Hamilton JA, Tang G, Dolnikowski GG, Vogel S, Duester G, Plutzky J.** 2007. Retinaldehyde represses adipogenesis and diet-induced obesity. Nat. Med. **13:**695–702.
6. **Zhang M, Hu P, Krois CR, Kane MA, Napoli JL.** 2007. Altered vitamin A homeostasis and increased size and adiposity in the *rdh1*-null mouse. FASEB J. **21:**2886–2896.
7. **Jeyakumar SM, Vajreswari A, Giridharan NV.** 2006. Chronic dietary vitamin A supplementation regulates obesity in an obese mutant WNIN/Ob rat model. Obesity **14:**52–59.
8. **Mercader J, Ribot J, Murano I, Felipe F, Cinti S, Bonet ML, Palou A.** 2006. Remodeling of white adipose tissue after retinoic acid administration in mice. Endocrinology **147:**5325–5332.
9. **Berry DC, DeSantis D, Soltanian H, Croniger CM, Noy N.** 2012. Retinoic acid upregulates preadipocyte genes to block adipogenesis and suppress diet-induced obesity. Diabetes **61:**1112–1121.
10. **Ribot J, Felipe F, Bonet ML, Palou A.** 2001. Changes of adiposity in response to vitamin A status correlate with changes of PPAR gamma 2 expression. Obes. Res. **9:**500–509.
11. **Bonet ML, Ribot J, Palou A.** 2012. Lipid metabolism in mammalian tissues and its control by retinoic acid. Biochim. Biophys. Acta **1821:**177–189.
12. **Yasmeen R, Jeyakumar SM, Reichert B, Yang F, Ziouzenkova O.** 2012. The contribution of vitamin A to autocrine regulation of fat depots. Biochim. Biophys. Acta **1821:**190–197.
13. **Safonova I, Darimont C, Amri EZ, Grimaldi P, Ailhaud G, Reichert U, Shroot B.** 1994. Retinoids are positive effectors of adipose cell differentiation. Mol. Cell. Endocrinol. **104:**201–211.
14. **Reichert B, Yasmeen R, Jeyakumar SM, Yang F, Thomou T, Alder H, Duester G, Maiseyeu A, Mihai G, Harrison EH, Rajagopalan S, Kirkland JL, Ziouzenkova O.** 2011. Concerted action of aldehyde dehydrogenases influences depot-specific fat formation. Mol. Endocrinol. **25:**799–809.
15. **Murray T, Russell TR.** 1980. Inhibition of adipose conversion in 3T3-L2 cells by retinoic acid. J. Supramol. Struct. **14:**255–266.
16. **Kuri-Harcuch W.** 1982. Differentiation of 3T3-F442A cells into adipocytes is inhibited by retinoic acid. Differentiation **23:**164–169.
17. **Kamei Y, Kawada T, Mizukami J, Sugimoto E.** 1994. The prevention of adipose differentiation of 3T3-L1 cells caused by retinoic acid is elicited through retinoic acid receptor alpha. Life Sci. **55:**PL307–PL312.
18. **Xue JC, Schwarz EJ, Chawla A, Lazar MA.** 1996. Distinct stages in adipogenesis revealed by retinoid inhibition of differentiation after induction of PPARgamma. Mol. Cell. Biol. **16:**1567–1575.
19. **Schwarz EJ, Reginato MJ, Shao D, Krakow SL, Lazar MA.** 1997. Retinoic acid blocks adipogenesis by inhibiting C/EBPbeta-mediated transcription. Mol. Cell. Biol. **17:**1552–1561.
20. **Marchildon F, St-Louis C, Akter R, Roodman V, Wiper-Bergeron NL.** 2010. Transcription factor Smad3 is required for the inhibition of adipogenesis by retinoic acid. J. Biol. Chem. **285:**13274–13284.
21. **Choy L, Derynck R.** 2003. Transforming growth factor-beta inhibits adipocyte differentiation by Smad3 interacting with CCAAT/enhancer-binding protein (C/EBP) and repressing C/EBP transactivation function. J. Biol. Chem. **278:**9609–9619.
22. **Sul HS, Smas CM, Wang D, Chen L.** 1998. Regulation of fat synthesis and adipose differentiation. Prog. Nucleic Acid Res. Mol. Biol. **60:**317–345.
23. **Heyman RA, Mangelsdorf DJ, Dyck JA, Stein RB, Eichele G, Evans RM, Thaller C.** 1992. 9-cis retinoic acid is a high affinity ligand for the retinoid X receptor. Cell **68:**397–406.
24. **Levin AA, Sturzenbecker LJ, Kazmer S, Bosakowski T, Huselton C, Allenby G, Speck J, Kratzeisen C, Rosenberger M, Lovey A, et al.** 1992. 9-cis retinoic acid stereoisomer binds and activates the nuclear receptor RXR alpha. Nature **355:**359–361.
25. **Canan Koch SS, Dardashti LJ, Cesario RM, Croston GE, Boehm MF, Heyman RA, Nadzan AM.** 1999. Synthesis of retinoid X receptor-specific ligands that are potent inducers of adipogenesis in 3T3-L1 cells. J. Med. Chem. **42:**742–750.
26. **Yamauchi T, Waki H, Kamon J, Murakami K, Motojima K, Komeda K, Miki H, Kubota N, Terauchi Y, Tsuchida A, Tsuboyama-Kasaoka N, Yamauchi N, Ide T, Hori W, Kato S, Fukayama M, Akanuma Y, Ezaki O, Itai A, Nagai R, Kimura S, Tobe K, Kagechika H, Shudo K, Kadowaki T.** 2001. Inhibition of RXR and PPARgamma ameliorates diet-induced obesity and type 2 diabetes. J. Clin. Invest. **108:**1001–1013.
27. **Fu M, Sun T, Bookout AL, Downes M, Yu RT, Evans RM, Mangelsdorf DJ.** 2005. A nuclear receptor atlas: 3T3-L1 adipogenesis. Mol. Endocrinol. **19:**2437–2450.
28. **Repa JJ, Hanson KK, Clagett-Dame M.** 1993. All-*trans*-retinol is a ligand for the retinoic acid receptors. Proc. Natl. Acad. Sci. U. S. A. **90:**7293–7297.
29. **Quadro L, Blaner WS, Salchow DJ, Vogel S, Piantedosi R, Gouras P, Freeman S, Cosma MP, Colantuoni V, Gottesman ME.** 1999. Impaired retinal function and vitamin A availability in mice lacking retinol-binding protein. EMBO J. **18:**4633–4644.
30. **Naylor HM, Newcomer ME.** 1999. The structure of human retinol-binding protein (RBP) with its carrier protein transthyretin reveals an interaction with the carboxy terminus of RBP. Biochemistry **38:**2647–2653.
31. **Berry DC, Croniger CM, Ghyselinck NB, Noy N.** 2012. Transthyretin blocks retinol uptake and cell signaling by the holo-retinol-binding protein receptor STRA6. Mol. Cell. Biol. **32:**3851–3859.
32. **Kawaguchi R, Yu J, Honda J, Hu J, Whitelegge J, Ping P, Wiita P, Bok D, Sun H.** 2007. A membrane receptor for retinol binding protein mediates cellular uptake of vitamin A. Science **315:**820–825.
33. **Kawaguchi R, Yu J, Ter-Stepanian M, Zhong M, Cheng G, Yuan Q, Jin M, Travis GH, Ong D, Sun H.** 2011. Receptor-mediated cellular uptake mechanism that couples to intracellular storage. ACS Chem. Biol. **6:**1041–1051.
34. **Ruiz A, Mark M, Jacobs H, Klopfenstein M, Hu J, Lloyd M, Habib S, Tosha C, Radu RA, Ghyselinck NB, Nusinowitz S, Bok D.** 2012. Retinoid content, visual responses, and ocular morphology are compromised in the retinas of mice lacking the retinol-binding protein receptor, STRA6. Invest. Ophthalmol. Vis. Sci. **53:**3027–3039.
35. **Pasutto F, Sticht H, Hammersen G, Gillessen-Kaesbach G, Fitzpatrick DR, Nurnberg G, Brasch F, Schirmer-Zimmermann H, Tolmie JL, Chitayat D, Houge G, Fernandez-Martinez L, Keating S, Mortier G, Hennekam RC, von der Wense A, Slavotinek A, Meinecke P, Bitoun P, Becker C, Nurnberg P, Reis A, Rauch A.** 2007. Mutations in STRA6 cause a broad spectrum of malformations including anophthalmia, congenital heart defects, diaphragmatic hernia, alveolar capillary dysplasia, lung hypoplasia, and mental retardation. Am. J. Hum. Genet. **80:**550–560.
36. **Alapatt P, Guo F, Komanetsky SM, Wang S, Cai J, Sargsyan A, Rodriguez Diaz E, Bacon BT, Aryal P, Graham TE.** 2013. Liver retinol transporter and receptor for serum retinol binding protein (RBP4). J. Biol. Chem. **288:**1250–1265.
37. **Blaner WS.** 2007. STRA6, a cell-surface receptor for retinol-binding protein: the plot thickens. Cell Metab. **5:**164–166.
38. **Yang Q, Graham TE, Mody N, Preitner F, Peroni OD, Zabolotny JM, Kotani K, Quadro L, Kahn BB.** 2005. Serum retinol binding protein 4 contributes to insulin resistance in obesity and type 2 diabetes. Nature **436:**356–362.
39. **Shirakami Y, Lee SA, Clugston RD, Blaner WS.** 2012. Hepatic metabolism of retinoids and disease associations. Biochim. Biophys. Acta **1821:**124–136.
40. **Kawaguchi R, Zhong M, Kassai M, Ter-Stepanian M, Sun H.** 2012. STRA6-catalyzed vitamin A influx, efflux, and exchange. J. Membr. Biol. **245:**731–745.
41. **Berry DC, Jin H, Majumdar A, Noy N.** 2011. Signaling by vitamin A and retinol-binding protein regulates gene expression to inhibit insulin responses. Proc. Natl. Acad. Sci. U. S. A. **108:**4340–4345.
42. **Berry DC, O'Byrne SM, Vreeland AC, Blaner WS, Noy N.** 2012. Cross talk between signaling and vitamin A transport by the retinol-binding protein receptor STRA6. Mol. Cell. Biol. **32:**3164–3175.
43. **Norseen J, Hosooka T, Hammarstedt A, Yore MM, Kant S, Aryal P, Kiernan UA, Phillips DA, Maruyama H, Kraus BJ, Usheva A, Davis RJ, Smith U, Kahn BB.** 2012. Retinol-binding protein 4 inhibits insulin signaling in adipocytes by inducing proinflammatory cytokines in macrophages through a c-Jun N-terminal kinase- and Toll-like receptor 4-dependent and retinol-independent mechanism. Mol. Cell. Biol. **32:**2010–2019.
44. **Xia M, Liu Y, Guo H, Wang D, Wang Y, Ling W.** 2013. Retinol binding protein 4 stimulates hepatic SREBP-1 and increases lipogenesis through PGC-1beta-dependent pathway. Hepatology **58:**564–575.

45. **Farjo KM, Farjo RA, Halsey S, Moiseyev G, Ma JX.** 2012. Retinol-binding protein 4 induces inflammation in human endothelial cells by an NADPH oxidase- and nuclear factor kappa B-dependent and retinol-independent mechanism. Mol. Cell. Biol. **32:**5103–5115.
46. **Schupp M, Lefterova MI, Janke J, Leitner K, Cristancho AG, Mullican SE, Qatanani M, Szwergold N, Steger DJ, Curtin JC, Kim RJ, Suh M, Albert MR, Engeli S, Gudas LJ, Lazar MA.** 2009. Retinol saturase promotes adipogenesis and is downregulated in obesity. Proc. Natl. Acad. Sci. U. S. A. **106:**1105–1110.
47. **Wilson CG, Schupp M, Burkhardt BR, Wu J, Young RA, Wolf BA.** 2010. Liver-specific overexpression of pancreatic-derived factor (PANDER) induces fasting hyperglycemia in mice. Endocrinology **151:**5174–5184.
48. **Schupp M, Cristancho AG, Lefterova MI, Hanniman EA, Briggs ER, Steger DJ, Qatanani M, Curtin JC, Schug J, Ochsner SA, McKenna NJ, Lazar MA.** 2009. Re-expression of GATA2 cooperates with peroxisome proliferator-activated receptor-{gamma} depletion to revert the adipocyte phenotype. J. Biol. Chem. **284:**9458–9464.
49. **Kawaguchi R, Sun H.** 2010. Techniques to study specific cell-surface receptor-mediated cellular vitamin A uptake. Methods Mol. Biol. **652:**341–361.
50. **Bouillet P, Sapin V, Chazaud C, Messaddeq N, Decimo D, Dolle P, Chambon P.** 1997. Developmental expression pattern of Stra6, a retinoic acid-responsive gene encoding a new type of membrane protein. Mech. Dev. **63:**173–186.
51. **Smas CM, Sul HS.** 1993. Pref-1, a protein containing EGF-like repeats, inhibits adipocyte differentiation. Cell **73:**725–734.
52. **Schulz TJ, Huang TL, Tran TT, Zhang H, Townsend KL, Shadrach JL, Cerletti M, McDougall LE, Giorgadze N, Tchkonia T, Schrier D, Falb D, Kirkland JL, Wagers AJ, Tseng YH.** 2011. Identification of inducible brown adipocyte progenitors residing in skeletal muscle and white fat. Proc. Natl. Acad. Sci. U. S. A. **108:**143–148.
53. **D'Ambrosio DN, Clugston RD, Blaner WS.** 2011. Vitamin A metabolism: an update. Nutrients **3:**63–103.
54. **Green H, Meuth M.** 1974. An established pre-adipose cell line and its differentiation in culture. Cell **3:**127–133.
55. **Teng M, Duong TT, Johnson AT, Klein ES, Wang L, Khalifa B, Chandraratna RA.** 1997. Identification of highly potent retinoic acid receptor alpha-selective antagonists. J. Med. Chem. **40:**2445–2451.
56. **Faraonio R, Galdieri M, Colantuoni V.** 1993. Cellular retinoic-acid-binding-protein and retinol-binding-protein mRNA expression in the cells of the rat seminiferous tubules and their regulation by retinoids. Eur. J. Biochem. **211:**835–842.
57. **Scherer PE, Williams S, Fogliano M, Baldini G, Lodish HF.** 1995. A novel serum protein similar to C1q, produced exclusively in adipocytes. J. Biol. Chem. **270:**26746–26749.
58. **Kawaguchi R, Yu J, Wiita P, Honda J, Sun H.** 2008. An essential ligand-binding domain in the membrane receptor for retinol-binding protein revealed by large-scale mutagenesis and a human polymorphism. J. Biol. Chem. **283:**15160–15168.
59. **Reznikoff CA, Bertram JS, Brankow DW, Heidelberger C.** 1973. Quantitative and qualitative studies of chemical transformation of cloned C3H mouse embryo cells sensitive to postconfluence inhibition of cell division. Cancer Res. **33:**3239–3249.
60. **Floyd ZE, Stephens JM.** 2003. STAT5A promotes adipogenesis in nonprecursor cells and associates with the glucocorticoid receptor during adipocyte differentiation. Diabetes **52:**308–314.
61. **Belatik A, Hotchandani S, Bariyanga J, Tajmir-Riahi HA.** 2012. Binding sites of retinol and retinoic acid with serum albumins. Eur. J. Med. Chem. **48:**114–123.
62. **Futterman S, Heller J.** 1972. The enhancement of fluorescence and the decreased susceptibility to enzymatic oxidation of retinol complexed with bovine serum albumin, lactoglobulin, and the retinol-binding protein of human plasma. J. Biol. Chem. **247:**5168–5172.
63. **Friebe D, Neef M, Erbs S, Dittrich K, Kratzsch J, Kovacs P, Bluher M, Kiess W, Korner A.** 2011. Retinol binding protein 4 (RBP4) is primarily associated with adipose tissue mass in children. Int. J. Pediatr. Obes. **6:**e345–e352.
64. **Henze A, Frey SK, Raila J, Tepel M, Scholze A, Pfeiffer AF, Weickert MO, Spranger J, Schweigert FJ.** 2008. Evidence that kidney function but not type 2 diabetes determines retinol-binding protein 4 serum levels. Diabetes **57:**3323–3326.
65. **Mody N, Graham TE, Tsuji Y, Yang Q, Kahn BB.** 2008. Decreased clearance of serum retinol-binding protein and elevated levels of transthyretin in insulin-resistant *ob*/*ob* mice. Am. J. Physiol. Endocrinol. Metab. **294:**E785–E793.
66. **Isken A, Golczak M, Oberhauser V, Hunzelmann S, Driever W, Imanishi Y, Palczewski K, von Lintig J.** 2008. RBP4 disrupts vitamin A uptake homeostasis in a STRA6-deficient animal model for Matthew-Wood syndrome. Cell Metab. **7:**258–268.
67. **Mills JP, Furr HC, Tanumihardjo SA.** 2008. Retinol to retinol-binding protein (RBP) is low in obese adults due to elevated apo-RBP. Exp. Biol. Med. **233:**1255–1261.
68. **Frey SK, Spranger J, Henze A, Pfeiffer AF, Schweigert FJ, Raila J.** 2009. Factors that influence retinol-binding protein 4-transthyretin interaction are not altered in overweight subjects and overweight subjects with type 2 diabetes mellitus. Metabolism **58:**1386–1392.
69. **Frey SK, Nagl B, Henze A, Raila J, Schlosser B, Berg T, Tepel M, Zidek W, Weickert MO, Pfeiffer AF, Schweigert FJ.** 2008. Isoforms of retinol binding protein 4 (RBP4) are increased in chronic diseases of the kidney but not of the liver. Lipids Health Dis. **7:**29.
70. **Tsutsumi C, Okuno M, Tannous L, Piantedosi R, Allan M, Goodman DS, Blaner WS.** 1992. Retinoids and retinoid-binding protein expression in rat adipocytes. J. Biol. Chem. **267:**1805–1810.
71. **Dani C, Smith AG, Dessolin S, Leroy P, Staccini L, Villageois P, Darimont C, Ailhaud G.** 1997. Differentiation of embryonic stem cells into adipocytes in vitro. J. Cell Sci. **110**(Part 11)**:**1279–1285.
72. **Bost F, Caron L, Marchetti I, Dani C, Le Marchand-Brustel Y, Binetruy B.** 2002. Retinoic acid activation of the ERK pathway is required for embryonic stem cell commitment into the adipocyte lineage. Biochem. J. **361:**621–627.
73. **Monteiro MC, Wdziekonski B, Villageois P, Vernochet C, Iehle C, Billon N, Dani C.** 2009. Commitment of mouse embryonic stem cells to the adipocyte lineage requires retinoic acid receptor beta and active GSK3. Stem Cells Dev. **18:**457–463.
74. **White JA, Beckett-Jones B, Guo YD, Dilworth FJ, Bonasoro J, Jones G, Petkovich M.** 1997. cDNA cloning of human retinoic acid-metabolizing enzyme (hP450RAI) identifies a novel family of cytochromes P450. J. Biol. Chem. **272:**18538–18541.
75. **Preitner F, Mody N, Graham TE, Peroni OD, Kahn BB.** 2009. Long-term fenretinide treatment prevents high-fat diet-induced obesity, insulin resistance, and hepatic steatosis. Am. J. Physiol. Endocrinol. Metab. **297:**E1420–E1429.
76. **McIlroy GD, Delibegovic M, Owen C, Stoney PN, Shearer KD, McCaffery PJ, Mody N.** 2012. Fenretinide treatment prevents diet-induced obesity in association with major alterations in retinoid homeostatic gene expression in adipose, liver and hypothalamus. Diabetes **62:**825–836.
77. **Aeberli I, Biebinger R, Lehmann R, L'Allemand D, Spinas GA, Zimmermann MB.** 2007. Serum retinol-binding protein 4 concentration and its ratio to serum retinol are associated with obesity and metabolic syndrome components in children. J. Clin. Endocrinol. Metab. **92:**4359–4365.
78. **Kim JY, van de Wall E, Laplante M, Azzara A, Trujillo ME, Hofmann SM, Schraw T, Durand JL, Li H, Li G, Jelicks LA, Mehler MF, Hui DY, Deshaies Y, Shulman GI, Schwartz GJ, Scherer PE.** 2007. Obesity-associated improvements in metabolic profile through expansion of adipose tissue. J. Clin. Invest. **117:**2621–2637.
79. **Lehmann JM, Moore LB, Smith-Oliver TA, Wilkison WO, Willson TM, Kliewer SA.** 1995. An antidiabetic thiazolidinedione is a high affinity ligand for peroxisome proliferator-activated receptor gamma (PPAR gamma). J. Biol. Chem. **270:**12953–12956.